DOI: 10.1002/ejic.200601234

Inter- and Intramolecular Electron Transfer in Modified Azurin Dimers

Thyra E. de Jongh,[a] Maren Hoffmann,[b] Oliver Einsle,[b] Davide Cavazzini,[c] Gian-Luigi Rossi,[c] Marcellus Ubbink,[a] and Gerard W. Canters*[a]

Keywords: Metalloproteins / Protein structures / Copper protein / Electronic coupling / Hydrophobic patch

A dimer of N42C azurin (*P. aeruginosa*), formed by intermolecular disulfide bond formation between the introduced surface-exposed cysteine residues, was previously shown to exhibit low rates of intramolecular electron self-exchange. The work presented here aims to render the construct sensitive to pH by the introduction of an additional surface mutation (M64E). The structural and mechanistic effects of ionisable residues in the hydrophobic patch were analysed as a function of pH. A crystal structure of the dimer at pH = 3.1, solved to 2.3 Å resolution, displays an orientation distinct from other known azurin complexes. The dimer exhibits slow intramolecular self-exchange at pH* = 4.5 ($k_{ese}^{intra} \approx 25\ s^{-1}$), in line with the Cu–Cu distance of 20.5 Å observed in the crystal structure of the dimer. The intermolecular electron self-exchange rate constant amounts to $k_{inter} = (1.8 \pm 0.1) \times 10^4\ M^{-1}s^{-1}$. Thus, at protein concentrations less than 1 mM, the intramolecular process dominates the electron self-exchange. A change from low to high pH results in a slowing down of the electron-exchange processes. A partitioning between intra- and intermolecular exchange proved impossible at low pH due to the limited precision of the experimental data.

Introduction

Abbreviations: 1,5-dip: 1,5-bis(imidazol-1-yl)pentane; 1,6-dih: 1,6-bis(imidazol-1-yl)hexane; wt: wild type; Azu: azurin; BMME: bis(maleimidomethyl) ether.

Among the physico-chemical processes that constitute the basis of life, the formation of protein–protein complexes occupies a prominent place. An example of this kind is provided by the metabolic processes in the living cell. They are mediated by protein–protein complexes that promote interprotein electron transfer (ET). These complexes have a transient nature. Their lifetimes reflect the rate at which metabolic processes take place in the cell and generally lie within the range of from 1 to 1000 ms. It is precisely their fleeting existence which makes these transient complexes difficult to study by conventional means such as crystallography. Two main alternative routes of research have been explored in the recent past. One technique relies on the use of NMR which is a form of spectroscopy that is eminently suited for the study of dynamic processes and short-lived structures.[1–4] The other is to freeze the complexes by covalently linking them as soon as they have formed in the hope that the covalently linked complex preserves the active conformation. The cross-linked complex can then be studied in detail.

Previous research has focused on complexes in which two monomers of the electron-transfer protein azurin (Azu) have been linked.[5,6] The rationale for studying these complexes is twofold. First, the covalent linking of the partners in an encounter complex may lead to a configuration that is different from the active configuration, i.e. the configuration that leads to protein–protein ET. For this reason it is important to study how the linking may affect the structure of the complex and how small changes in the contact surface may influence the details of this structure. Secondly, it is of interest to know how the structure of the complex and thereby the ET process may be modified by applying changes in the surface of the contact area. This may be relevant for the technological implementation of proteins in electronic devices such as sensors, actuating elements and fuel cells etc.

Azurin from *Pseudomonas aeruginosa* is a so-called blue copper protein of 14 kDa, in which a single Cu ion is immobilized in the protein structure through bonds to two histidines, a cysteine and a methionine. The backbone carbonyl oxygen atom of a glycine completes the coordination shell through a weak coordinate bond. The electron self-exchange (ese) rate of the protein is high ($1 \times 10^6\ M^{-1}s^{-1}$, at room temperature) and insensitive to pH.[7] The crystal

[a] Leiden Institute of Chemistry, Leiden University, Gorlaeus Laboratories,
P. O. Box 9502, 2300 RA Leiden, The Netherlands
Fax: +31-71-527-4349
E-mail: canters@chem.leidenuniv.nl
URL: http://www.chem.leidenuniv.nl/metprot
[b] Institut für Mikrobiologie und Genetik, Georg-August-Universität Göttingen
Justus-von-Liebig-Weg 11, 37077 Göttingen, Germany
[c] Department of Biochemistry and Molecular Biology, University of Parma
V.le G. P. Usberti 23/A., 43100 Parma, Italy
Supporting information for this article is available on the WWW under http://www.eurjic.org or from the author.

structure of Azu provides a clue as to why the ese rate is so high.[8] The Azu molecules pack with their so-called hydrophobic patches positioning the His117 ligands of the Cu atoms in the monomers directly opposite each other.[8] This configuration optimises the electronic coupling between the Cu centres in the two monomers. The coupling is further enhanced by the presence of two water molecules that form an H-bonded pathway between the N^{ε} atoms of the two histidines.[8,9]

Confirmation that this is a favoured orientation for two Azu molecules in an ET-active complex came from studies of complexes in which two Azu molecules were covalently linked. By introducing a cysteine at position 42 (Asn42Cys mutation) and incubating the mutated protein with bis(maleimidomethyl) ether (BMME), a covalently linked dimer of Azu was obtained in which the hydrophobic patches face each other.[5] A high intramolecular ese rate was observed ($>10^4\ s^{-1}$) while the intermolecular rate (i.e. between two different dimers) was too slow to be measurable.[5] The latter observation confirmed that the packing of the Azu moieties in the dimer blocks the hydrophobic patch, thereby rendering intermolecular ET virtually impossible. Leaving out the BMME linker and connecting the two Azu molecules directly by the Cys42–Cys42 disulfide bridge resulted in a complex in which the two Azu molecules had rotated around the Cys42 –Cys42 link, apparently to relieve a slight steric hindrance. As a result intra-ese stopped. Inter-ese was only slightly slower than observed for wild-type (wt) Azu.[5,6]

Earlier evidence for the involvement of the hydrophobic patch in the ese reaction of (monomeric) azurin had been obtained from studies of azurin variants in which charges had been introduced in the hydrophobic patch. The Met44-Lys mutation, for instance, was found to diminish the ese rate by two orders of magnitude in the pH range in which the Lys side chain is protonated and therefore charged, while the ese rate returns to its wt value at high pH, at which the Lys side chain becomes deprotonated and therefore uncharged.[10–12] Likewise, the Met64Glu mutation caused a slowing down of the ese reaction at high pH where the Glu side chain becomes charged.[13]

The present study deals with Azu dimers that are linked directly through a Cys–Cys link at position 42. In addition, a charge was introduced in the hydrophobic patch by the mutation M64E. The effect of pH on the inter- and intra-dimer electron self-exchange was studied. The expectation was that the inter-dimer ese rate would be affected by pH while, by analogy with earlier results on the Cys42–Cys42-coupled dimer, the intra-protein rate would be too slow to be measurable and independent of pH. Contrary to this expectation, the latter rate appeared to be clearly non-zero. Also, the structure of the complex as determined by X-ray diffraction shows that the two Azu moieties are in an orientation that differs from both the BMME- and the disulfide-linked dimers of the N42C Azu variant. NMR spectroscopic studies substantiate the absence of significant structural variations in time, as well as the absence of significant perturbations of the interface between the two monomers. The observed rates can be rationalised with the help of current models of ET on the basis of the observed structure of the complex. The results show that our present understanding of the parameters that determine the structure of an association complex is insufficient to predict structural variations on the basis of simple intuitive arguments.

Results

Electron self-exchange rates were determined by monitoring the resolved NMR signal of the $H^{\gamma 2}$ methyl group of Val31. In oxidised wt Azu, this signal occurs at δ = –0.77 ppm at room temperature and pH = 8.5, while it occurs at δ = –0.69 ppm in reduced Azu. In a partly reduced/partly oxidised solution of Azu, two signals can therefore be observed at –0.77 and –0.69 ppm, which coalesce in the case when there is fast electron self-exchange between reduced and oxidized Azu, while only broadening of the individual signals is seen when the ese is slow. By analysing the shape of the Val31 γ2-methyl signal the ese rate can be extracted. Repeating the measurements at a series of different pH values gives the pH dependence of the ese rate.

For wt Azu, the position of the Val31 signal is pH-dependent.[12] At low pH the signal occurs at δ = –0.670 and –0.720 ppm for reduced and oxidised Azu, respectively, while at high pH these positions are δ = –0.690 and –0.770 ppm, respectively. At intermediate pH values the peaks of both the high- and the low-pH forms can be seen simultaneously, their relative intensities varying with pH. This is illustrated in Figure 1A. Apparently, the protein is involved in a protonation/deprotonation equilibrium with slow exchange kinetics. It is known that the residue involved is His35.[11,12,14] The pH dependence of the Val31 signals, with different pK_a values for the oxidised and reduced forms (Figure 1B), complicates the analysis of the electron self-exchange data considerably. Therefore, His35 was eliminated by replacing it with phenylalanine. This is one of a series of His35 mutations which are known only to marginally affect the structure of the Azu and its ET kinetics.[11,15] It was checked that the H35F mutation eliminated the pH dependence of the Val31 resonances (Figure 1A).

For the next experiments, Azu was prepared in which the following mutations had been applied: His35Phe, Asn42Cys and Met64Glu. Subsequently, dimers were constructed in which the Azu moieties were connected through the C42–C42 S–S bridge. In solutions of partly reduced/oxidised dimers broadening but no coalescence of the Val31 γ2-methyl signals was observed when compared with signals from the fully reduced or oxidised solutions (Figure 2). Qualitatively it can be concluded that the exchange is in the slow regime.

To distinguish the contributions to the line broadening that derive from inter-dimer and intra-dimer electron self-exchange, the Val31 γ2-methyl signals were measured as a function of total concentration of the dimer. One would expect the *intra*-dimer contribution to be constant and the *inter*-dimer contribution to diminish at lower concentrations. The signals measured at pH* = 4.5 and 295 K (Fig-

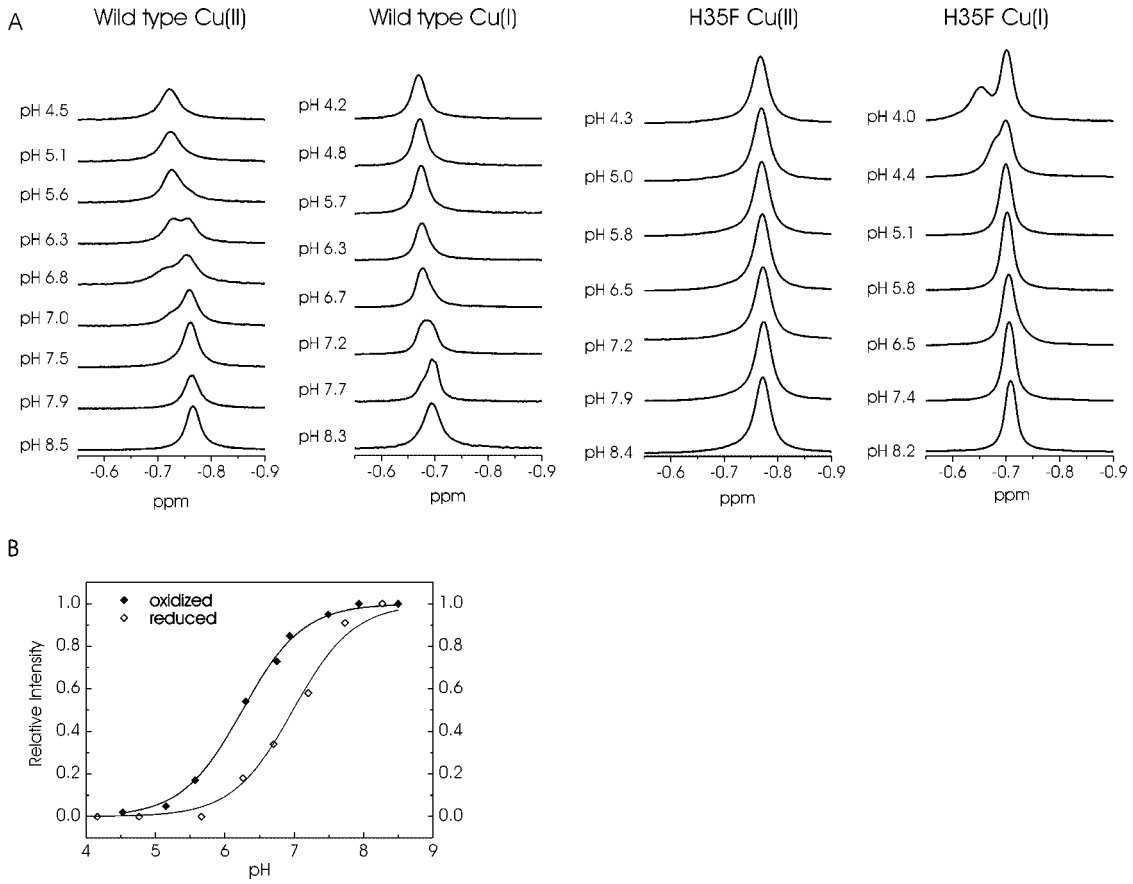

Figure 1. A. Upfield region of the ^{1}H NMR spectrum of oxidised and reduced wt azurin (left) and His35Phe azurin (right) showing the Val31 $^1H^{\gamma 2}$ resonance at various pH values. The extra peak developing in the spectrum of reduced H35F azurin towards low pH is due to the start of denaturation. B. Normalised integrated intensity of the high-pH resonance of Cu^{II} (filled diamonds) and Cu^{I} (open diamonds) wt azurin vs. pH. Solid lines represent fits to the Henderson–Hasselbalch equation from which $pK_{a,ox}$ and $pK_{a,red}$ were determined at 6.3 and 7.0, respectively.

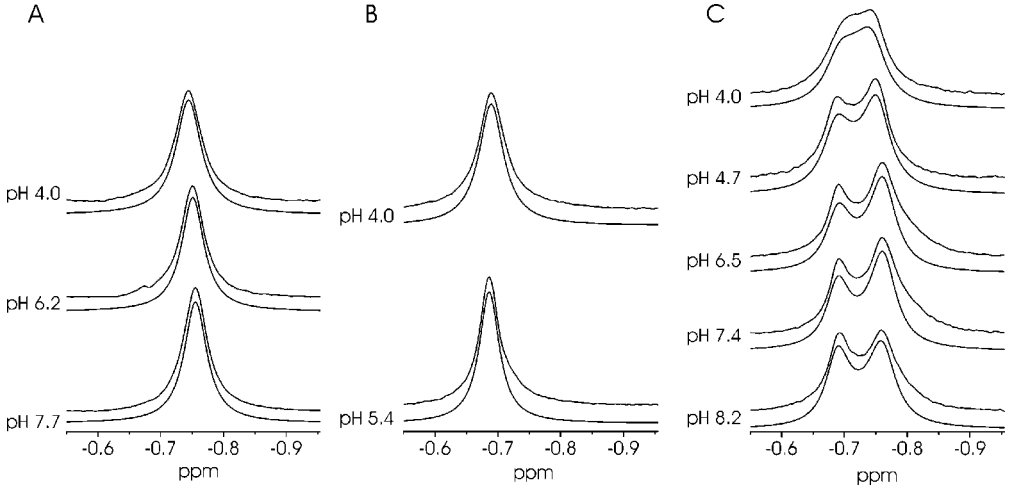

Figure 2. Val31 γ2-methyl resonance in the ^{1}H NMR spectrum of H35F/N42C/M64E disulfide azurin at (A) 100%, (B) 0% and (C) 50–60% oxidation (1 mM of dimer protein in 25 mM potassium phosphate, T = 295 K). The upper traces represent the experimental data, while the simulated spectra generated using the MEX software program are shown in the lower traces. The experimental spectra have been corrected for the presence of a small (≈ 5%) amount of redox-inactive azurin with a resonance at δ ≈ –0.69 ppm.

ure 3A) were simulated with the MEX/MEXICO software.[16] The input parameters consisted of the line widths and positions of the signals measured at the highest and lowest dilution for the 100% *ox* and 100% *red* solutions. The inter- and intramolecular electron self-exchange rates were varied until the best fit with experiment was obtained.

The fits are reproduced in Figure 3A and the observed rates as a function of dimer concentration are shown in Figure 3B. The intra-dimer contribution is constant, as expected, and corresponds to an intra-dimer ese rate of k_{intra} = 25 s^{-1}. The inter-dimer contribution is proportional to the concentration. The slope yields the second-order rate constant which amounts to $k_{inter} = (1.8 \pm 0.1) \times 10^4$ $M^{-1} s^{-1}$.

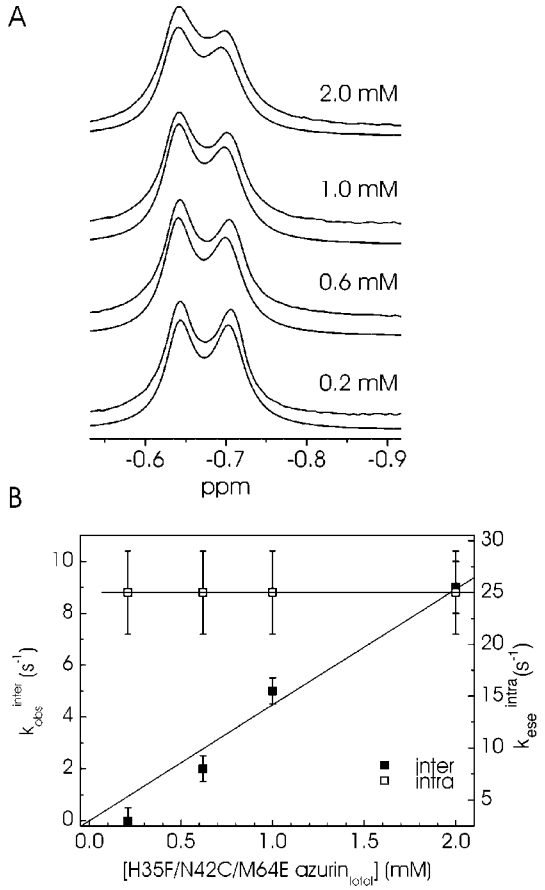

Figure 3. A. Upfield region of the ^{1}H NMR spectrum of H35F/N42C/M64E disulfide azurin at (50 ± 3) % oxidation at several dilutions. The upper traces show the experimental data, the MEX-simulated spectra are shown in the lower traces (T = 295 K, 25 mM potassium phosphate, pH* = 4.5). B. k_{obs}^{inter} (filled squares) and k_{ese}^{intra} (open squares) values for H35F/N42C/M64E disulfide azurin that correspond to the simulated traces shown in panel A vs. the protein dimer concentration. The lines indicate least-squares linear fits.

The next question to be addressed deals with the pH dependence of the line broadening. It is clear from Figure 2C that the broadening becomes less at high pH, indicating that the electron self-exchange processes slow down in a similar way to that observed for the monomeric species in solution.[13] Simulation with the MEX software shows that the combined contributions from the intra- and inter-electron self-exchange processes decrease by a factor of 3 when going from pH = 4.0 to 8.2. The partitioning between these two processes was not possible. This was because of insufficient precision of the data resulting from the difficulty in keeping the degree of oxidation/reduction of the solution precisely fixed during the pH titration.

To aid in the interpretation of the data, the structure of the N42C/M64E azurin S–S dimer at pH = 3.1 was determined to 2.3 Å resolution by X-ray diffraction. The results are presented in Table 1. Crystals obtained at high pH did not diffract well enough for structure analysis. The structure of the dimer is shown in Figure 4B. For comparison the packing of the monomers in the crystal of wt Azu is shown in Figure 4A.[8] In Figure 4C the C42–C42-connected dimer of Azu is depicted in which no other than the N42C mutation had been applied.[5] It is clear that in Figure 4C the two halves of the dimer have rotated around the Cys–Cys link when compared with Figure 4A. Remarkably, the structure in Figure 4B is intermediate.

Table 1. Data collection and refinement statistics.

Space group	$P2_12_12$
Unit cell	a = 68.57 Å
	b = 116.98 Å
	c = 30.29 Å
Molecules in asymmetric unit[a]	2
Resolution limits	60.0–2.3 Å
Independent reflections	10369
Completeness (last shell)	95.1% (95.6%)
R_{merge} (last shell)	0.095 (0.060)
$I/\sigma(I)$ (last shell)	8.3 (2.4)
R_{cryst} (R_{free})	0.208 (0.281)
r.m.s.d. bonds	0.034
r.m.s.d. angles	2.843

[a] Molecules seen as monomeric azurin subunits.

Comparison of each of the subunits of the N42C/M64E azurin dimer with the structure of reduced wt azurin at pH = 5.5 (PDB access code 1E5Y) shows that they are largely unaffected by the introduction of the mutations. The overall backbone atom root-mean-square difference between the wt structure and each of the monomers in the N42C/M64E dimers amounts to 0.6 Å, excluding the N- and C-terminal residues. The regions directly around the sites of the mutation are relatively unperturbed. The two subunits share a contact surface, with the contacts between the two surfaces consisting mainly of weak hydrophobic interactions in a manner that is clearly distinct from the classical hydrophobic packing in crystals of wt azurin.[8] In the dimer interface, two water molecules can be found that form several hydrogen bonds with the protein (Figure 5). A hydrogen-bonding network across the interface is formed which stabilises the conformation of the dimer by forming hydrogen bonds between each of the water molecules to Glu64 O^{ε} or the backbone oxygen atoms of Cys42 on both protein chains. The shortest Cu–Cu distance observed is the intramolecular distance of 20.5 Å. All Cu–Cu distances between dimers in adjacent asymmetric units within the crystal exceed 25 Å. These intermolecular interactions can therefore be considered irrelevant for the electron self-exchange analysis.

To probe the dynamic aspects of the dimer structure, HSQC NMR spectra were obtained for the ^{15}N-labelled dimer and compared with those of the ^{15}N-labelled monomer. The spectra were measured at a number of pH values (Supporting Information: Figure S2). The dimer spectra are al-

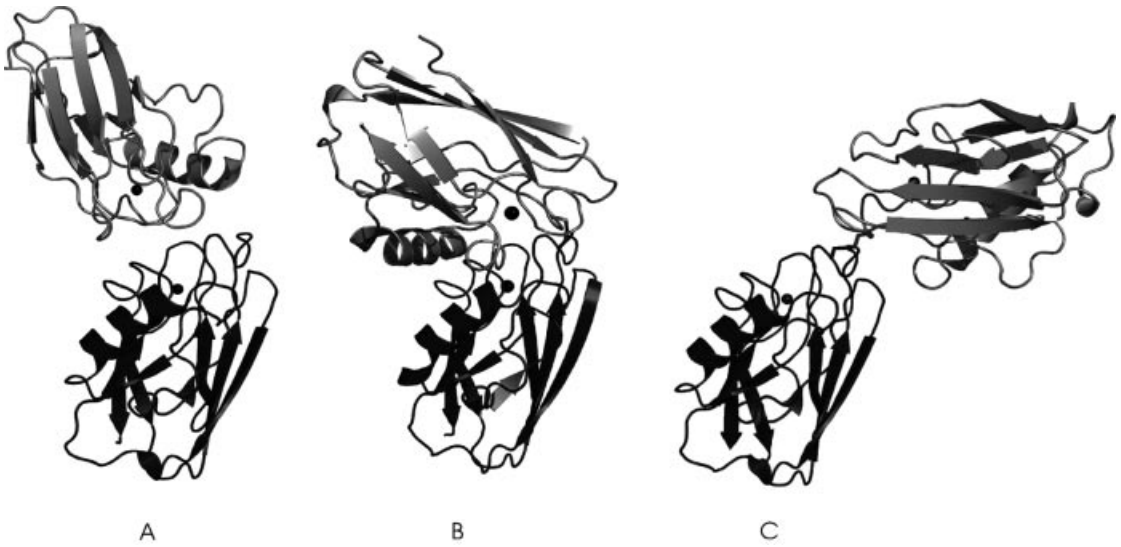

Figure 4. A. Packing of two molecules of reduced wt azurin from *Pseudomonas aeruginosa* in the crystal structure of the protein at pH = 5.5; data from pdb entry 1E5Y. B. Structure of the Cys42–Cys42-linked dimer of azurin carrying in each monomer the mutations Asn42Cys and Met64Glu. The Cu centres are oxidised; pH = 3.1; data from pdb entry 2OJ1. C. Structure of the Cys42–Cys42-linked dimer of azurin carrying in each monomer the mutations Asn42Cys. The Cu centres are oxidised; pH = 8.5; data from pdb entry 1JVO.

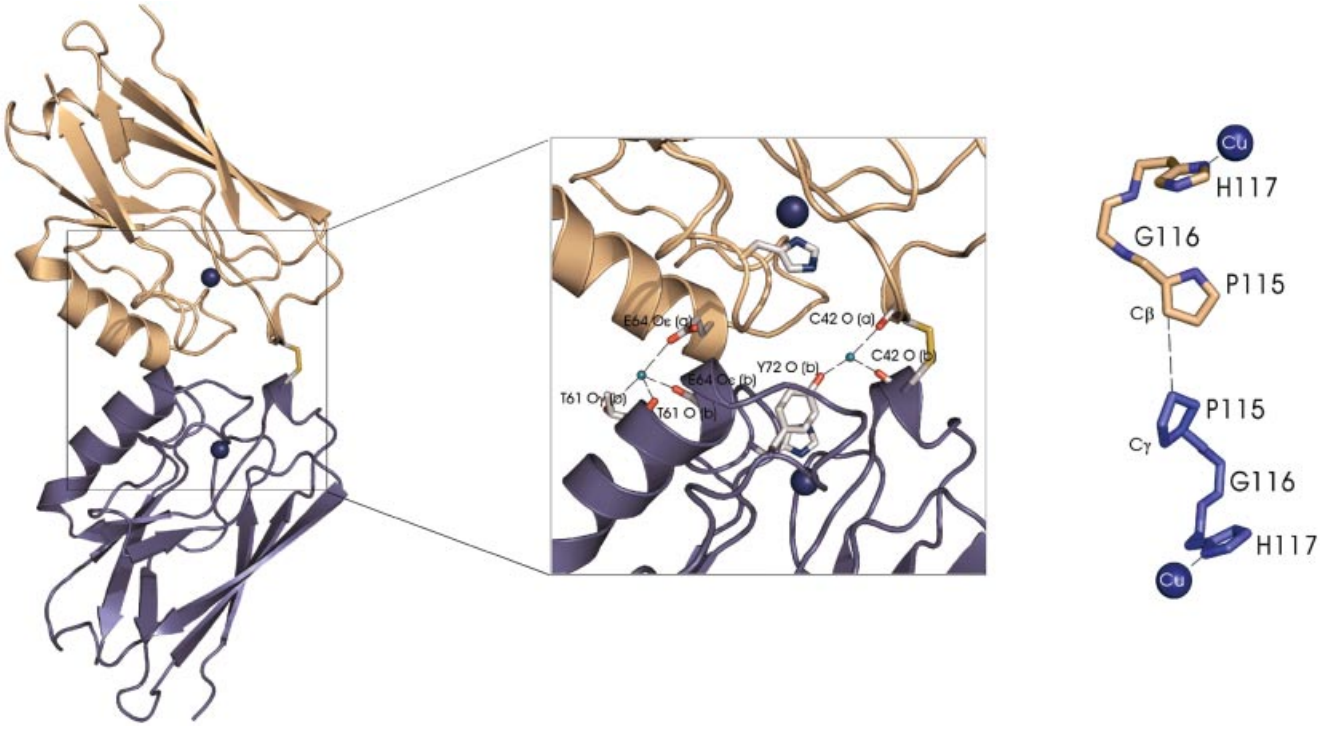

Figure 5. Left: Crystal structure of the N42C/M64E azurin disulfide-bridged dimer at pH = 3.1. The copper centres are depicted as dark-blue spheres. Close-up: Interface of the dimer showing the ordered water molecules (small light-blue spheres). All residues involved in hydrogen bonding with these water molecules are shown (sticks) and labelled. The hydrogen bonds are shown as dashed lines. The letters within parentheses indicate the individual protein chains (a and b). Also shown are the Cu ligands H117 (sticks). Right: Tunnelling pathway between the copper centres of the N42C/M64E disulfide-bridged dimer of azurin as calculated with the programme HARLEM.[22] The through-space jump between Pro115(A) C-β and Pro115(B) C-γ is indicated by a dashed line.

most identical to those of the monomer except for a few residues in the hydrophobic patch, viz. C42, V43 and M44. When increasing the pH from 4.4 to 8.4 the cross peaks corresponding to these residues move to slightly different positions (Figure S2). The transition occurs at a somewhat lower pH for the dimer. There is no evidence for strong interactions between the subunits since, overall, no severe perturbations of the resonance patterns can be observed.

Discussion

The aim of the work presented here was to construct a protein complex with pH-dependent structural and ET properties. To this end, a covalently cross-linked homodimer of the blue copper protein azurin was created by intermolecular disulfide bond formation between engineered surface-exposed cysteines. The pH dependence was introduced by substitution of the interfacial M64 by an ionisable Glu residue. Analysis of the ET rate as a function of pH required additional replacement of the protonatable H35 residue by Phe. It was shown that over the entire pH range studied, the complex exhibited slow electron self-exchange. Although no unambiguous distinction could be made between the inter- and intramolecular contributions to the ese process from the pH-dependent data, the concentration dependence of the observed ese rate identifies intramolecular exchange as the dominant process (see Figure 3).

Despite the presence of several ionisable groups in the interface, the electron self-exchange behaviour of the complex shows only moderate pH dependence. The low exchange rates observed for the H35F/N42C/M64E dimer (1.8×10^4 M^{-1} s^{-1}) contrast with what is observed for the N42C azurin dimer for which a roughly ten times higher k_{ese}^{inter} was determined (2.8×10^5 M^{-1} s^{-1}). It is tempting to relate this difference to the clear difference between the crystallographically determined structures of the two complexes. Whereas the N42C dimer adopts a rather "open" dimer conformation [interfaces are $a = (1.8 \times 10^2)$ Å^2] with an intramolecular Cu–Cu distance >25 Å, the N42C/M64E dimer at pH = 3.1 forms a much more closed conformation [interfaces are $a = (7.0 \times 10^2)$ Å^2] in which the straight intramolecular Cu–Cu distance is only 20.5 Å. Although this distance is still rather large, it is within the limits that allow for intramolecular e.s.e., albeit with low rates. The alternative explanation that in the H35F/N42C/M64E dimer the Glu64 unit in the interface is deprotonated and therefore intermolecular association is slowed down, is less likely since at the employed pH* of 4.5 the ese rate of the monomer is not yet affected by deprotonation of Glu64.[13]

According to Dutton et al., the rate of ET, k_{ET}, between two redox centres separated by a homogeneous medium is given by Equation (1),[17,18] in which ρ denotes the packing density, d the distance separating the donor and acceptor sites, λ the reorganization energy and ΔG^0 the standard free energy of the reaction (energies are in eV).

$$\log k_{ET} = 13.0 - (1.2 - 0.8\rho)(d - 3.6) - (\Delta G^0 + \lambda)^2/\lambda \quad (1)$$

For the N42C azurin dimer, these parameters are λ = 0.7 eV, ρ = 0.75 and ΔG^0 = 0 eV (e.s.e.).[5] Based on these parameters and a Cu–Cu distance of 20.5 Å, a value of $k_{ese}^{intra} \approx 1.4 \times 10^2$ s^{-1} can be predicted, in reasonable agreement with the experimentally determined rate.

Alternatively, ET can be viewed as proceeding along defined tunnelling pathways (TPs).[19–22] In the crystal structure of the N42C/M64E dimer a path can be identified that involves residues H117, G116 and P115 on both chains and a large through-space jump of 4.0 Å between the C-β and C-γ atoms of Pro115 on either chain, respectively (Figure 5). The coupling efficiency of this pathway is extremely low ($\Pi_\varepsilon < 10^{-8}$) and is, in fact, too low for ET to occur at a discernible rate. The pathway algorithm, however, calculates couplings in static structures with fixed distances between atoms. In reality, protein motions may temporarily shorten through-space distances, increasing the coupling strength. Also, although in the crystal structure no ordered water molecules were observed within hydrogen-bonding distances of the P115 residues, in solution solvent molecules may temporarily contribute to the electronic coupling and enhance the electron self-exchange.

Conclusions

Chemical shift perturbation analysis of the dimer indicates that the dimer interface is not strongly perturbed by the covalent linking of the monomers throughout the investigated pH range. Also, contrary to expectation, the neutralisation of the Glu64 side chain has little effect on the conformation of the dimer. The crystal structure of the dimer at low pH shows, again contrary to expectation, that the two Azu moieties in the dimer move less far apart (through a rotation around the Cys42–Cys42 link) than in the dimer without the M64E mutation.

The observed ese rates are in accordance with the structural features. The intermolecular rate is lower than in the C42–C42 dimer without the M64E mutation, in agreement with the smaller surface accessible area in the hydrophobic patch. The intramolecular ese rate on the other hand is larger, in line with the smaller Cu–Cu distance.

The phenomenological model of Dutton et al. gives a value for the ese rate that is in accordance with observation whereas the pathway model of Beratan, Betts and Onuchic predicts a rate that is orders of magnitude too small because there is a gap in the pathway that has to be bridged. It means that the structure may have dynamic features, by which the gap is closed some of the time; although, on a millisecond time scale, the NMR spectroscopic data provide no indication for time-dependent features of the dimer structure within the investigated pH range. Alternatively, water molecules may bridge the gap as seen in several other dimer-like structures of Azu. No water molecules could be observed in the structure suggesting that there are no ordered water molecules in the interface. However, this does not necessarily mean that in the course of time they cannot provide effective electronic coupling.

The overall conclusion is that the ET rates and the structural data produce a consistent picture of the Azu (N42C/M64E) dimer that is clearly different from simple intuition. Why the N42C/M64E Azu dimer behaves counter-intuitively remains open to further experimentation.

Experimental Section

Mutagenesis: The secondary mutation M64E was introduced into the N42C azurin gene by splice overlap extension (SOE) site-directed mutagenesis for which two partially complementary oligo-

nucleotides were designed. The forward primer (i.e. extending in the coding direction) 5′-*GGGCGTGCTCAC*CGACGGC**GA**-GGCTTCCG encodes for the replacement of methionine-64 by a glutamate. The reverse primer 5′-*GTGACCACGCCC*-TGCATGTC**T**GC**A**GCGGTGCT includes two silent mutations that encode a *Pst*I restriction site for screening purposes. The section in *italics* shows the complimentary regions in the two primers, the mutation sites are shown in bold. As a template, the N42C azu containing plasmid pIA02, derived from pUC18, was used.[6] The presence of the N42C/M64E azurin gene in the newly created plasmid pTJ01 was confirmed by sequence analysis and the obtained plasmid was then used as a template for the one-step synthesis of the H35F/N42C/M64E azurin gene in a procedure based on the Stratagene's ExSite® PCR-Based Site-Directed Mutagenesis Kit. Two fully complementary 32 base-pair-long oligonucleotides encoding the His35Phe mutation were used as primers: (forward primer) 5′-CCGTCAACCTGTCC**TTC**CCCGG*G*AACC-TGCCG. The mutated codon for the H35F substitution is indicated in bold and an additional silent mutation that was introduced for screening by *Xma*I digestion is in *italics.* Sequence analysis confirmed the presence of all desired mutations in the resultant pTJ02 plasmid. The H35F/N42C/M64E azurin gene was subcloned into a pET28a vector for cytoplasmic expression by removal of the signal sequence. Gene amplification was performed using primers for *N*-terminal signal peptide removal (5′-GGTCAGCG*CCATGG*CCGAGTGC TCGGTGG (*Nco*I site is in *italics*) and addition of a *C*-terminal *Bam*HI/*Bst*YI recognition site (in *italics*) (5′-CCGA*GGATCC*GCATCACTTCAGGG). Insertion into a pET28a vector was accomplished by digestion of the gene fragment using the restriction enzymes *Bst*YI and *Nco*I. The vector was digested by the enzymes *Bam*HI and *Nco*I, after which the gene and vector fragments were ligated resulting in the plasmid named pTJ13.

Protein Expression and Purification: Wild-type and H35F azurin were expressed and produced as described previously.[11,23] Non-isotopically labelled N42C/M64E azurin and H35F/N42C/M64E azurin were produced in the periplasmic space of *E. coli* JM109 cells transformed with plasmids pTJ01 or pTJ02, respectively. Cells were cultured on an LB medium at 37 °C/250 rpm to an OD_{600} of 0.6 before induction by addition of 100 μM IPTG. Cells were harvested by centrifugation typically about 5 h after induction. Both mutants were isolated and purified from the medium as described for N42C azurin with yields of 10–15 mg/L.[6] Up to 50% of the purified azurin was found to contain zinc in the metal-binding site and was thus redox-inactive. Uniformly ^{15}N-labelled H35F/N42C/M64E azurin was produced in the cytoplasm of BL21 *E. coli* cells transformed with pTJ13 and grown on isotopically labelled OD2-N medium (Silantes GmbH) supplemented with 50 μM kanamycin at 30 °C/200 rpm. Once an OD_{600} of 0.5 was obtained, the temperature was lowered to 25 °C followed by induction with 1 mM IPTG after 30 min. Due to lower growth rates, cells grown on the OD2-N medium were not harvested until 15 h after induction. The cytoplasmically produced protein was released from the cells by resuspension in 20 mM MES, 100 mM NaCl, pH = 6.5 and disruption of the cells in a French Press cell in the presence of phenylmethylsulfonyl fluoride (PMSF) (1 mM) and DNase I (50 mg mL^{-1}). After centrifugation, the protein was isolated from the resultant supernatant following a protocol similar to that used for periplasmically expressed azurin. The protein was initially purified in the apo form and reconstituted with copper before further purification on a DEAE ion exchange column.

Cross Linking: Disulfide-linked dimers of N42C/M64E and H35F/N42C/M64E holo-azurin were spontaneously formed upon addition of a slight molar excess of $Cu(NO_3)_2$ and an approximately five-fold excess of $K_3Fe(CN)_6$. Excess $Cu(NO_3)_2$ and $K_3Fe(CN)_6$ were subsequently removed by repeated rounds of dilution and concentration using a Centricon concentration device (Molecular weight cut-off: 10 kDa). Analysis of the protein sample by SDS-PAGE under non-reducing conditions showed near complete dimerization.

NMR Sample Preparation: Fully reduced samples were obtained by incubation with 2 mM ascorbate at room temp. until the sample had turned completely colourless. Ascorbate was then removed from the sample by washing with deaerated 25 mM potassium phosphate (KP_i) at pH = 7.0. All NMR samples of unlabelled protein were prepared in 25 mM KP_i at pH* = 7.0 (* uncorrected for deuterium isotope effect), 99.9% D_2O and concentrated to 1–2 mM of protein. For experiments in which the protein concentration had to be varied, the sample was stepwise diluted with 25 mM KP_i at pH* = 7.0 until dilution by a factor of 10 was reached. The pH of the samples was adjusted to the desired value by addition of small amounts of NaOD or DCl. Partially oxidised samples were attained by mixing of fully oxidised and fully reduced protein in the required ratios. The degree of oxidation of the samples was determined by measuring the absorbance at 628 nm relative to a fully oxidised sample of the same concentration. UV/Vis spectra were recorded with a Perkin–Elmer lambda 800 spectrophotometer using a special sample holder for NMR tubes equipped with fibre-optic light guides (Hellma). A sample of fully reduced, monomeric ^{15}N-H35F/N42C/M64E azurin was prepared in 25 mM KP_i at pH = 5.7, 5 mM dithiotreitol (DTT) supplemented with 6% D_2O and concentrated to 2 mM. The pH of the sample was adjusted by addition of small amounts of NaOH or HCl. After recording the NMR spectra, DTT was removed by repeated rounds of concentration and dilution with 25 mM KP_i. Dimerisation of the protein was accomplished by addition of a catalytic amount of $Cu(NO_3)_2$ and an approximately ten-fold molar excess of $K_3Fe(CN)_6$. Once fully dimerised, as confirmed by SDS-PAGE analysis, the protein was transferred to a solution containing 25 mM KP_i at pH = 4.3. Selective reduction to Cu^I azurin without disruption of the intermolecular disulfide bond was performed by addition of 2 mM ascorbate. Titration to the desired pH was achieved by addition of small amounts of either NaOH or HCl.

NMR Spectroscopy: All ^{1}H NMR experiments were performed at 295 K with a Bruker Avance DMX 600 MHz spectrometer. Spectra were calibrated against an internal reference of 200 μM 3-(trimethylsilyl)propionate-d_4 (TSP). As the chemical shift of TSP (δ) is sensitive to pH (pK_a = 5.0), its reference position was corrected for pH according to Equation (2).[24]

$$\delta = 0.003 - 0.019 \times (1 + 10^{(5.0-pH)})^{-1} \quad (2)$$

In addition to the Val31 ^{1}H signal of the oxidised protein, the spectra of the fully oxidised samples indicated the presence of a small amount (≈ 5%) of an additional species for which a low-intensity resonance was observed at δ ≈ –0.69 ppm at all pH values. This feature is commonly encountered in samples of azurin and can be attributed to the presence of a small amount of redox-inactive azurin. This resonance was subtracted from the experimental spectra shown in Figure 2. Multi-dimensional NMR experiments were performed at 302 K. Data sets were processed in the AZARA program suite (available at http://www.bio.cam.ac.uk) and analysed with ANSIG for WINDOWS 1.0.[25,26] Backbone assignments were obtained through standard sequential assignment procedures using the [^{15}N,^{1}H] HSQC, NOESY-HSQC and TOCSY-HSQC spectra on the basis of assignments available for wild-type azurin.[27]

Electron Self-Exchange Rate Determination: The ese rates were determined by simulation of the line shape of the Val31 methyl ^{1}H NMR resonance using the MEX/MEXICO program suite developed by Bain and Duns.[16] All possible intermolecular and intramolecular exchange processes were taken into account (see Supporting Information). The chemical shifts and linewidths of the fully oxidised and fully reduced protein were given as input parameters whilst both the inter- and intramolecular ese rates were manually iterated until simulations were obtained that resembled the experimental traces best, as judged by visual inspection.

Crystallisation and Structure Solution: The disulfide-linked dimer of N42C/M64E azurin was crystallised by sitting drop vapour diffusion using a reservoir solution containing 30% (w/v) polyethylene glycol 4000 and 0.1 M sodium citrate buffer at pH = 3.1. The protein was concentrated to 8 mg mL^{-1} and mixed in a 1:1 ratio with the reservoir solution. Rod-shaped crystals grew within 2 d. Due to the high content of PEG 4000, the mother liquor turned out to be sufficiently cryoprotective for direct flash-cooling of the crystals in liquid nitrogen without formation of ice. Data were collected with a Rigaku MicroMax 007 rotating-anode X-ray generator with a mar345dtb image plate detector. For structure solution, the model of the native azurin from *P. aeruginosa* was used with the program MOLREP. Two monomers were found in the asymmetric unit, clearly connected through a disulfide bridge between residues 42. The N42C and M64E mutations were modelled with O,[28] and refinement was carried out with REFMAC5.[29] The coordinates and structure factors have been deposited in the Protein Data Bank under accession code 2OJ1. Figures 4 and 5 were generated using PyMOL 0.98.[30]

Solvent Accessibility and Interface Areas: The solvent-accessible surface area (ASA) was calculated using the program NACCESS 2.1.1 with a probe radius of 1.4 Å. The interface area was defined as the sum of the ASAs of the individual proteins minus the ASA of the complex. The interface in disulfide-bridged dimers of N42C azurin was defined as the average of the two dimers in the asymmetric unit of the structure deposited in the protein data bank with accession code 1JVO.[6]

Supporting Information (see footnote on the first page of this article): This material contains, first, a description of the model used as a basis for the lineshape simulations. The simulations were used to determine the electron self-exchange rates for the azurin dimer. Second, it contains the 2D-NMR data as a function of pH obtained on the H35F/N42C/M64E azurin monomers and the H35F/N42C/M64E azurin dimers.

[1] P. B. Crowley, M. Ubbink, *Acc. Chem. Res.* **2003**, *36*, 723–730.
[2] M. Prudêncio, M. Ubbink, *J. Mol. Recognit.* **2004**, *17*, 524–539.
[3] M. Ubbink, *Photosynth. Res.* **2004**, *81*, 277–287.
[4] A. N. Volkov, J. A. R. Worrall, E. Holtzmann, M. Ubbink, *Proc. Natl. Acad. Sci. USA* **2006**, *103*, 18945–18950.
[5] I. M. C. van Amsterdam, M. Ubbink, O. Einsle, A. Messerschmidt, A. Merli, D. Cavazzini, G. L. Rossi, G. W. Canters, *Nat. Struct. Biol.* **2002**, *9*, 48–52.
[6] I. M. C. van Amsterdam, M. Ubbink, L. J. C. Jeuken, M. P. Verbeet, O. Einsle, A. Messerschmidt, G. W. Canters, *Chem. Eur. J.* **2001**, *7*, 2398–2406.
[7] C. M. Groeneveld, G. W. Canters, *Eur. J. Biochem.* **1985**, *153*, 559–564.
[8] H. Nar, A. Messerschmidt, R. Huber, M. van de Kamp, G. W. Canters, *J. Mol. Biol.* **1991**, *221*, 765–772.
[9] K. V. Mikkelsen, L. K. Skov, H. Nar, O. Farver, *Proc. Natl. Acad. Sci. USA* **1993**, *90*, 5443–5445.
[10] M. van de Kamp, G. W. Canters, C. R. Andrew, J. Sanders-Loehr, C. J. Bender, J. Peisach, *Eur. J. Biochem.* **1993**, *218*, 229–238.
[11] M. van de Kamp, M. C. Silvestrini, M. Brunori, J. van Beeumen, F. C. Hali, G. W. Canters, *Eur. J. Biochem.* **1990**, *194*, 109–118.
[12] M. van de Kamp, Thesis, Leiden University, **1993**.
[13] G. van Pouderoyen, S. Mazumdar, N. I. Hunt, H. A. O. Hill, G. W. Canters, *Eur. J. Biochem.* **1994**, *222*, 583–588.
[14] M. C. Silvestrini, M. Brunori, M. T. Wilson, V. M. Darleyusmar, *J. Inorg. Biochem.* **1981**, *14*, 327–338.
[15] H. Nar, A. Messerschmidt, R. Huber, M. van de Kamp, G. W. Canters, *J. Mol. Biol.* **1991**, *218*, 427–447.
[16] A. D. Bain, G. J. Duns, *Can. J. Chem.* **1996**, *74*, 819–824.
[17] C. C. Moser, C. C. Page, X. Chen, P. L. Dutton, *J. Biol. Inorg. Chem.* **1997**, *2*, 393–398.
[18] C. C. Moser, J. M. Keske, K. Warncke, R. S. Farid, P. L. Dutton, *Nature* **1992**, *355*, 796–802.
[19] D. N. Beratan, J. N. Onuchic, J. N. Winkler, H. B. Gray, *Science* **1992**, *258*, 1740–1741.
[20] D. N. Beratan, J. N. Onuchic, J. J. Hopfield, *J. Chem. Phys.* **1987**, *86*, 4488–4498.
[21] D. N. Beratan, J. N. Betts, J. N. Onuchic, *Science* **1991**, *252*, 1285–1288.
[22] I. V. Kurnikov, D. N. Beratan, *J. Chem. Phys.* **1996**, *105*, 9561.
[23] M. van de Kamp, F. C. Hali, N. Rosato, A. F. Agro, G. W. Canters, *Biochim. Biophys. Acta* **1990**, *1019*, 283–292.
[24] D. S. Wishart, C. G. Bigam, J. Yao, F. Abildgaard, H. J. Dyson, E. Oldfield, J. L. Markley, B. D. Sykes, *J. Biomol. NMR* **1995**, *6*, 135–140.
[25] M. Helgstrand, P. Kraulis, P. Allard, T. Hard, *J. Biomol. NMR* **2000**, *18*, 329–336.
[26] P. J. Kraulis, *J. Magn. Reson.* **1989**, *84*, 627–633.
[27] M. van de Kamp, G. W. Canters, S. S. Wijmenga, A. Lommen, C. W. Hilbers, H. Nar, A. Messerschmidt, R. Huber, *Biochemistry* **1992**, *31*, 10194–10207.
[28] T. A. Jones, J. Y. Zou, S. W. Cowan, M. Kjeldgaard, *Acta Crystallogr., Sect. A* **1991**, *47*, 110–119.
[29] S. Bailey, *Acta Crystallogr., Sect. D* **1994**, *50*, 760–763.
[30] W. L. DeLano, *The PyMOL Molecular Graphics System*, San Carlos, CA, USA **2002**, http://www.pymol.org

Received: December 22, 2006
Published Online: May 8, 2007

